Original Article

Metabolic heterogeneity in different subtypes of malformations of cortical development causing epilepsy: a proton magnetic resonance spectroscopy study

Huaxia Pu[1#], Liping Wang[1#], Wenyu Liu[2#], Qiaoyue Tan[1], Xinyue Wan[3], Weina Wang[4], Xiaorui Su[1], Huaiqiang Sun[1], Simin Zhang[1], Qiang Yue[5,6], Qiyong Gong[1,7,8]

[1]Department of Radiology and Huaxi MR Research Center (HMRRC), West China Hospital of Sichuan University, Chengdu, China; [2]Department of Neurology, West China Hospital of Sichuan University, Chengdu, China; [3]Department of Radiology, Huashan Hospital, Fudan University, Shanghai, China; [4]Department of Radiology, The First Affiliated Hospital, College of Medicine, Zhejiang University, Hangzhou, China; [5]Department of Radiology, West China Hospital of Sichuan University, Chengdu, China; [6]Functional and Molecular Imaging Key Laboratory of Sichuan Province, West China Hospital of Sichuan University, Chengdu, China; [7]Department of Radiology, West China Xiamen Hospital of Sichuan University, Xiamen, China; [8]Research Unit of Psychoradiology, Chinese Academy of Medical Sciences, Chengdu, China

Contributions: (I) Conception and design: H Pu, L Wang, Q Yue, Q Gong; (II) Administrative support: Q Yue, Q Gong, H Sun; (III) Provision of study materials or patients: W Liu, Q Tan, X Wan, W Wang; (IV) Collection and assembly of data: W Wang, X Su, S Zhang, H Sun; (V) Data analysis and interpretation: H Pu, L Wang, Q Tan, X Wan, Q Yue; (VI) Manuscript writing: All authors; (VII) Final approval of manuscript: All authors.

[#]These authors contributed equally to this work.

Correspondence to: Qiang Yue, MD, PhD. Department of Radiology, West China Hospital of Sichuan University, No. 37 Guoxue Alley, Chengdu 610041, China; Functional and Molecular Imaging Key Laboratory of Sichuan Province, West China Hospital of Sichuan University, Chengdu 610041, China. Email: scu_yq@163.com; Qiyong Gong, MD, PhD. Department of Radiology and Huaxi MR Research Center (HMRRC), West China Hospital of Sichuan University, Chengdu 610041, China; Department of Radiology, West China Xiamen Hospital of Sichuan University, No. 699 Jinyuan Xi Road, Jimei District, Xiamen 361000, China; Research Unit of Psychoradiology, Chinese Academy of Medical Sciences, Chengdu, China. Email: qiyonggong@hmrrc.org.cn.

Background: The most common subtypes of malformations of cortical development (MCDs) are gray matter heterotopia (GMH), focal cortical dysplasia (FCD), and polymicrogyria (PMG). This study aimed to characterize the possible neurometabolic abnormalities and heterogeneity in different MCDs subtypes using proton magnetic resonance spectroscopy (^{1}H-MRS).

Methods: In this prospective cross-sectional study, we recruited 29 patients with MCDs and epilepsy, including ten with GMH, ten with FCD, and nine with PMG, as well as 25 age- and sex-matched healthy controls (HC) from the Epilepsy Center of West China Hospital of Sichuan University between August 2018 and November 2021. Inclusion criteria for the patients were based upon typical magnetic resonance imaging (MRI) findings of MCDs and full clinical assessment for epilepsy. Single-voxel point-resolved spectroscopy was used to acquire data from both the lesion and the normal-appearing contralateral side (NACS) in patients and from the frontal lobe in HC. Metabolite measures, including N-acetyl aspartate (NAA), myoinositol (Ins), choline (Cho), creatine (Cr), and glutamate + glutamine (Glx) concentrations, were quantitatively estimated with linear combination model (LCModel) software and corrected for the partial volume effect of cerebrospinal fluid (CSF).

Results: The NAA concentration was lower and the Ins concentration was higher in the MCDs lesions than in the NACS and in HC (P=0.002–0.007), and the Cho and Cr concentrations were higher in MCDs lesions than in HC (P=0.001–0.016). Moreover, the Cho concentration was higher in NACS than in HC (P=0.015). In the GMH lesions, the only metabolic alteration was an NAA reduction (GMH_lesion *vs.* HC:

P=0.001). In the FCD lesions, there were more metabolite abnormalities than in the other two subtypes, particularly a lower NAA and a higher Ins than in HC and NACS (P=0.012–0.042). In the PMG lesions, Cr (lesion *vs.* HC or NACS: P=0.017–0.021) and Glx (lesion *vs.* NACS: P=0.043) were increased, while NAA was normal. Correlation analysis revealed that the Cr concentration in MCDs lesions was positively correlated with seizure frequency (r=0.411; P=0.027).

Conclusions: Based upon ^{1}H-MRS, our study demonstrated that different MCDs subtypes exhibited variable metabolic features, which may be associated with distinct functional and cytoarchitectural properties.

Keywords: Malformations of cortical development (MCDs); proton magnetic resonance spectroscopy (^{1}H-MRS); gray matter heterotopia (GMH); focal cortical dysplasia (FCD); polymicrogyria (PMG)

Submitted Apr 21, 2023. Accepted for publication Sep 19, 2023. Published online Oct 16, 2023.
doi: 10.21037/qims-23-552
View this article at: https://dx.doi.org/10.21037/qims-23-552

Introduction

Malformations of cortical development (MCDs) are an inhomogeneous group of central nervous system developmental disorders resulting from the embryological interruption of any developmental stage, that is, during neuroblast proliferation and differentiation, neuronal migration, or cortical organization (1). These critical steps can be negatively affected by either genetic or acquired factors (2). MCDs are widely recognized as common and important causes of intractable epilepsy. Approximately 25–40% of drug-resistant childhood epilepsy cases are attributable to MCDs, and at least 75% of patients with MCDs will develop epilepsy (3). Barkovich *et al.* (4) described the updated version of the MCDs classification scheme in 2012. MCDs were categorized into the following three successive and partially overlapping groups: group I, malformations secondary to abnormal neuronal and glial proliferation or apoptosis, such as microcephaly; group II, malformations secondary to abnormal neuronal migration, such as gray matter heterotopia (GMH); and group III, malformations secondary to abnormal postmigrational development, such as focal cortical dysplasia (FCD) and polymicrogyria (PMG). GMH, PMG, and FCD are the most common MCDs subtypes.

Proton magnetic resonance spectroscopy (^{1}H-MRS) studies permit the noninvasive quantitative assessment of various cerebral metabolites implicated in cerebral structure and function *in vivo*. ^{1}H-MRS has been widely performed to evaluate the characterization of the metabolic state in normal brain as well as in various neurologic pathologic conditions (5). Previous MRS studies have examined metabolite ratios or metabolite concentrations in patients with MCDs as a population. Although the majority of these researches have reported a decrease in the neuronal marker N-acetyl aspartate (NAA) or the NAA to creatine (NAA/Cr) ratio, some studies have indicated normal or increased NAA in GMH (6,7) and PMG (7). Other metabolites, such as choline (Cho), Cr, Cho/Cr ratio, and myoinositol (Ins), etc., showed different changes across studies (6,8-13). We therefore suspect that the population of patients with MCDs was heterogeneous across these studies, as MCDs were divided into three groups. Also, the study by Woermann *et al.* (9) suggested there to be metabolic heterogeneity among the different subtypes of MCDs. In a previous study by our team, it was revealed that the disorders of migration (DOM) subgroup of MCDs was characterized by decreased NAA, while the disorders of postmigration (DOPM) subgroup was characterized by increased Ins (13). Munakata *et al.* (6) reported that the metabolic properties of the band heterotopia below the normotopic cortex differed from those of other cortical dysplasias.

In addition, several studies have discovered biochemical metabolic abnormalities in the perilesional area or normal-appearing contralateral side (NACS) (13-15), mainly in the form of NAA reduction. Functional magnetic resonance imaging (MRI) and diffusion tensor imaging (DTI) studies have confirmed that MCDs is a widespread disease that is not limited to the visible range of the lesion (16,17). This may explain why patients with a visible focal MCDs are less likely to obtain postsurgical seizure freedom after surgical resection of the entire lesion (18).

Given the differences in genetic, histopathological, and imaging characteristics across various subtypes of MCDs, we hypothesized that the differences in metabolic abnormalities can be expected to reflect this heterogeneity,

a suspicion that has not been extensively investigated in related researches. In this study, we aimed to detect the metabolic characteristics of the MCDs and NACS using a localized single-voxel ^{1}H-MRS technique; to assess the metabolic heterogeneity in GMH, FCD, and PMG; and to determine the correlations between metabolite levels and seizure duration or frequency. We hope to provide deeper insights into the pathophysiologic basis of epileptogenesis which may help the pharmacological or surgical management of different MCDs subtypes. We present this article in accordance with the STROBE reporting checklist (available at https://qims.amegroups.com/article/view/10.21037/qims-23-552/rc).

Methods

Participants

From August 2018 to November 2021, we prospectively enrolled 54 patients with epilepsy presenting with MCDs (including the GMH, FCD, and PMG groups) at the Epilepsy Center of West China Hospital of Sichuan University. The inclusion criteria for the patients was a clinically established diagnosis based on typical radiographic findings of MCDs and full clinical assessment (e.g., seizure semiology and video-electroencephalography). Conventional visual analysis of MRI was performed by two neuroradiologists in consensus. On MRI imaging, GMH is characterized by a nodular or laminar shape isointense to gray matter on all MRI sequences located in anywhere between the subependymal region of the lateral ventricles and cerebral cortex, without contrast enhancement (1). According to the distribution pattern of heterotopia, GMH is usually classified into subcortical laminar heterotopia (band heterotopia), subcortical nodular heterotopia, and subependymal/periventricular nodular heterotopia (1). FCD was identified according to the International League Against Epilepsy (ILAE) criteria, which include focal increased cortical thickness with abnormal signal intensity, the blurring of the gray-white matter junction, and increased subcortical white matter signal on T2-weighted images (T2WIs) and T2-fluid-attenuated inversion recovery (T2-FLAIR) images (19). On the MRI images of PMG, the lesion appears as an area of thickened and irregular cortex with multiple small gyri separated by shallow sulci on the cortical surface and often with abnormal subjacent white matter (1). The exclusion criteria for patients were as follows: (I) diffuse lesion, mixed MCDs subtypes, other MCDs subtypes, or other intercranial lesions; (II) any history of brain surgery or trauma; (III) alcohol/drug abuse or history of any other neurological or psychiatric disease except epilepsy; (IV) incomplete MR data; (V) poor spectral quality; and (VI) MRI contraindications.

Meanwhile, 25 age- and sex-matched healthy controls (HC) were also examined with the same protocol. Because there were 10 younger patients (age range, 7–15 years) in the MCDs group, the ethical problem of heavily sedating these patients prevented us from establishing a control group with the same age range. Therefore, in this study, we compared the MRS signal of the lesion with that of the NACS to overcome substantial regional (20) and age-dependent (21) variations in healthy brain spectra, and no remarkable differences between the two hemispheres are known (22). All HC had normal MRI findings on visual inspection. This study was approved by the local ethical committee of the West China Hospital of Sichuan University. Before scans, all participants or the legal guardians of younger patients provided written informed consent for enrollment in this study. The study was conducted in accordance with the Declaration of Helsinki (as revised in 2013).

Collected clinical data included the age at enrollment, age at seizure onset, duration of epilepsy, seizure frequency, the use of antiepileptic drugs, and location of the lesions on MRI.

MRI acquisition

The images for all participants were obtained on a 3.0-T MR scanner (Trio Tim, Siemens Healthcare, Erlangen, Germany) with an 8-channel phased array head coil. First, we used a magnetization-prepared rapid gradient echo (MPRAGE) sequence to acquire sagittal high-resolution T1-weighted images (T1WIs) [repetition time/echo time (TR/TE), 1,900/2.3 ms; matrix size, 256×256; field of view (FOV), 256 mm × 256 mm; slice thickness, 1 mm]. The axial and coronal images were then reconstructed based on sagittal images to acquire 3-dimensional localization of the spectral volumes of interest (VOIs).

Single-voxel ^{1}H-MRS acquisitions were conducted using the point-resolved spectroscopy sequence (PRESS) under the following parameters: TR/TE, 2,000/30 ms; the number of averages, 128; and bandwidth, 1,200 Hz. For each patient, a VOI was placed at the lesion and was adjusted to fit the size of the lesion to include as much of the visible lesion as possible, and an identically sized VOI

was positioned in the mirror region of the normal-appearing brain tissue in the contralateral hemisphere (i.e., the NACS) as a control volume. The average size of the VOIs was 9.3 mL (range, 4–16 mL). In the controls, the VOIs were centered on the symmetrical areas of the left and right frontal lobes, with a typical size of 12 mL (4.0×2.0×1.5 cm^3). For all participants, care was taken to ensure that VOIs did not involve the skull, subcutaneous fat of the scalp, or cerebrospinal fluid (CSF) spaces. Outer volume pre-saturation bands were placed to avoid interference from signals outside the VOIs. Spectra with and without water suppression were both acquired. Water suppression was achieved by three chemical shift-selective (CHESS) pulses prior to the PRESS module. Shimming was performed to obtain a smaller line width and a better signal-to-noise ratio (SNR).

Before enrollment, all patients underwent clear lesion localization via clinical conventional MRI. If there were any uncertainties, additional sequences (such as T2WI and T2-FLAIR) were performed to localize the MCDs lesions.

Data postprocessing

All raw MRS data were processed using the linear combination model (LCModel; version 6.3-1H; http://s-provencher.com/lcmodel.shtml), which has automated baseline and phase correction and yields the absolute metabolite concentrations using the tissue water signal as an internal reference (23). Two researchers examined the data carefully (Pu H and Wang L). Only spectra that met the following conditions were included in the subsequent analysis: SNR ≥10, full width at half maximum (FWHM) ≤0.08 ppm, and metabolite concentrations with an estimation of uncertainty [expressed as Cramer-Rao lower bounds (CRLB)] <15%. Neurometabolites selected for further analysis included NAA, Ins, Cho, Cr, and glutamate + glutamine (Glx). The final metabolite concentration unit was mole per kilogram (mmol/kg) wet weight.

To eliminate the partial volume effect of CSF, we used the cortical thickness procedure, advanced normalization tools (ANTs; https://stnava.github.io/ANTs/) to segment the T1WIs of all participants to obtain the whole-brain proportions of the gray matter, white matter, and CSF. The voxel CSF volume fraction was determined by overlaying the VOIs on the segmented T1WIs according to its location information (*Figure 1*) (23). Finally, the following formula was used to the calculate metabolite concentrations (corrected for CSF volume) (24): $C_{cor} = C_{raw} \times [V_{total}/(V_{total} - V_{CSF})]$, where C_{cor} is the corrected result, C_{raw} is the uncorrected result, V_{total} represents the total volume of the VOIs, and V_{CSF} represents the volume of CSF within the VOIs.

Statistical analysis

All statistical analyses were performed using SPSS 26 (IBM Corp., Armonk, NY, USA) and GraphPad Prism 9.0 (GraphPad Software, La Jolla, CA, USA). The Shapiro-Wilk test was used to test the normality of distribution of the data. The nonnormally distributed metabolites were analyzed via nonparametric tests, including the Wilcoxon, Mann-Whitney *U*, and Kruskal-Wallis tests. We compared age using the independent-samples *t*-test and examined the sex distribution using the chi-squared test. The paired *t*-test and Wilcoxon test were applied to test the difference in metabolite concentrations between the lesion and NACS in patients with MCDs as a population (only Glx was analyzed with the Wilcoxon test) or in each subtype (only the Cho and Glx of GMH were analyzed with the Wilcoxon test). The independent-samples *t*-test and the Mann-Whitney *U* test (including for comparing Ins, Cr, and Glx between the NACS of patients with MCDs and HC and comparing the Cho and Cr between the lesions of patients with MCDs and HC) were used to assess the significant differences between patients with MCDs and HC (average metabolite value of the bilateral frontal lobe). Kruskal-Wallis analyses (for comparing Ins and Cr between groups) and one-way analysis of variance (ANOVA) were performed among HC and the three MCDs subtypes. *Post-hoc* tests were performed using least-significant difference (LSD) or Tamhane's T2 as correction for multiple comparisons. Finally, Pearson's or Spearman's correlation coefficient was used to analyze the relationship between the metabolite concentrations and seizure frequency and between the metabolite concentrations and epilepsy duration. The significance level was set at a two-sided P value <0.05.

Results

A total of 29 patients with MCDs (12 females and 17 males; median age, 22.34 years; range, 7–41 years) met the inclusion criteria. The flowchart of the excluded patients with MCDs can be seen in *Figure 2*. The MCDs group consisted of 10 patients with GMH (female:male ratio =3:7; four with focal subcortical, three with subependymal, and three with unilateral subependymal

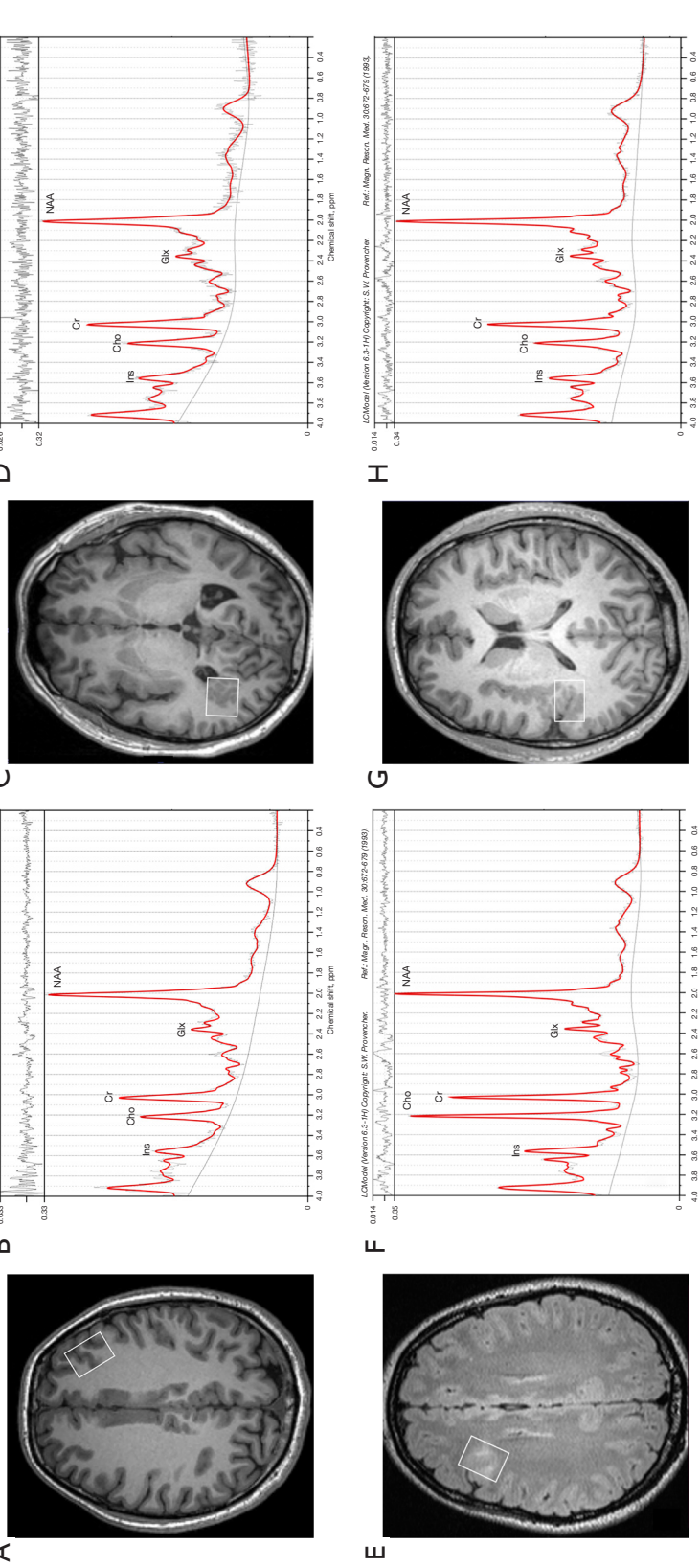

Figure 1 Axial T1WIs (A,C,G) or T2-FLAIR (E) and corresponding single-voxel ^{1}H-MRS in HC (A,B) and patients with GMH (C,D), FCD (E,F), and PMG (G,H) (23). The white box represents the spectral ROI in the left frontal lobe of a HC or the lesions from which the proton spectra are acquired. (B) Spectrum of a HC; the metabolite concentrations (the estimated value by the LCModel and the CSF corrected value) (mmol/kg wet weight) are as follows: Ins =4.38 and 4.75, NAA =7.26 and 7.87, Cho =1.39 and 1.51, Cr =5.13 and 5.56, and Glx =9.33 and 10.09. (D) Spectrum of a GMH lesion; the metabolite concentrations are as follows: Ins =4.99 and 5.17, NAA =6.81 and 7.06, Cho =1.42 and 1.47, Cr =6.08 and 6.30, and Glx =9.91 and 10.27. (F) Spectrum of a FCD lesion; the metabolite concentrations are as follows: Ins =5.94 and 6.43, NAA =6.35 and 6.86, Cho =2.56 and 2.77, Cr =6.31 and 6.83, and Glx =10.11 and 10.93. (H) Spectrum of a PMG lesion; the metabolite concentrations are as follows: Ins =5.22 and 5.77, NAA =7.89 and 8.73, Cho =1.30 and 1.44, Cr =5.74 and 6.34, and Glx =8.73 and 9.65. LCModel, linear combination model; Ins, myoinositol; Cho, choline; Cr, creatine; Glx, glutamate + glutamine; NAA, N-acetyl aspartate; T1WI, T1-weighted image; T2-FLAIR, T2-fluid-attenuated inversion recovery; ^{1}H-MRS, proton magnetic resonance spectroscopy; HC, healthy controls; GMH, gray matter heterotopia; FCD, focal cortical dysplasia; PMG, polymicrogyria; ROI, region of interest; CSF, cerebrospinal fluid.

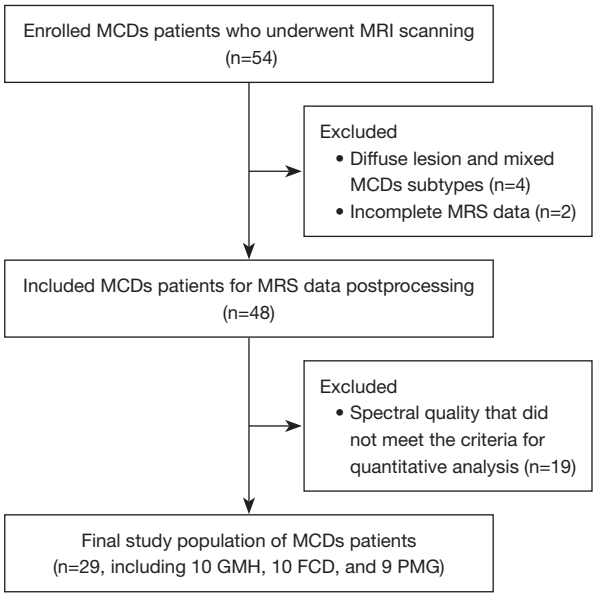

Figure 2 Flowchart of the inclusion of patients with MCDs in this study. MCDs, malformations of cortical development; MRI, magnetic resonance imaging; MRS, magnetic resonance spectroscopy; GMH, gray matter heterotopia; FCD, focal cortical dysplasia; PMG, polymicrogyria.

and subcortical heterotopia), ten patients with focal FCD (female:male ratio =6:4; seven with frontal and three with parietal FCD), and 9 patients with PMG (female:male ratio =3:6; two with focal frontal or parietal PMG; five with unilateral frontoparietal, temporal, or/and occipital PMG; two with bilateral focal parietooccipital PMG). Additionally, 25 sex- and age-matched HC (11 males and 14 females; mean age, 24.84 years; range, 22–28 years) were enrolled. The demographic and clinical characteristics of patients with MCDs are summarized in *Table 1*. We divided the patients into three subgroups: GMH, FCD, and PMG. There were no significant differences in age or sex among the HC group and the three subgroups (all P values >0.05). In terms of clinical features, the comparison results of the three subgroups showed that patients with FCD had a longer epilepsy duration than patients with GMH (12.50±9.66 *vs.* 4.30±4.30 years, P=0.042). Patients with PMG had a higher seizure frequency than patients with GMH (32.50±41.98 *vs.* 4.05±5.02 times/year, P=0.041).

Representative spectra and corresponding axial T1-weighted or T2-FLAIR images of HC and three MCDs subtypes are shown in *Figure 1*. *Table 2* summarizes the spectral quality (FWHM and SNR) and the tissue fractions in measured VOIs. The results showed that the MCDs lesions had higher FWHM and lower SNR than the NACS of MCDs (P=0.038 and P=0.001). The ratio of gray matter volume (GMV) to total volume and that of GMV to the sum of GMV and white matter volume (WMV) were higher, while the ratio of WMV to total volume and that of WMV to the sum of GMV and WMV was lower in HC than in lesion and NACS of MCDs (all P values <0.05). However, no significant differences in the spectral quality measurements between patients with MCDs and HC or in the tissue fractions of VOIs between the lesion and the NACS in MCDs were found (all P values >0.05). *Table 3* displays the metabolite concentrations of the patients and the HC expressed as mean ± standard deviation (mmol/kg wet weight). In addition, before using the average of the bilateral frontal metabolite concentrations in the HC group, we compared the metabolite concentrations between the left and right frontal lobes. The results showed that there were no significant metabolic differences between the two VOIs (P=0.073–0.663).

Metabolic differences among the lesion and NACS of MCDs, and the HC

Figure 3 shows the mean and range of metabolite concentrations in the lesion of MCDs, the NACS of MCDs, and the HC. The comparison between lesion and HC revealed that the NAA concentration was decreased (6.79±1.00 *vs.* 7.47±0.50, P=0.002), while the concentrations of Ins (5.67±1.53 *vs.* 4.82±0.49, P=0.007), Cho (1.63±0.39 *vs.* 1.38±0.10, P=0.001), and Cr (6.11±0.94 *vs.* 5.57±0.46, P=0.016) were increased in the lesion. In the comparison between lesion and the NACS, lower NAA (6.79±1.00 *vs.* 7.40±1.05, P=0.005) and higher Ins (5.67±1.53 *vs.* 4.77±0.85, P=0.003) concentrations were observed in the lesion. In the comparison between NACS and HC, only the Cho concentration was elevated in the NACS (1.52±0.29 *vs.* 1.38±0.10, P=0.015).

Metabolic differences between NACS and lesion in each MCDs subgroup

We performed intraindividual comparisons (paired *t*-test or Wilcoxon test) between the lesion and the NACS in each MCDs subtype, the results of which are displayed in *Figure 4*. In the patients with GMH, there was no significant difference in metabolite concentrations between

Table 1 Clinical data of patients with MCDs

Type	Case	Sex	Age (years)	Duration of epilepsy (years)	Seizure frequency (times/year)	Antiepileptic drugs
GMH	1	M	18	1	3	LEV, OXC, VPA
	2	M	9	7	Total 2	LEV, OXC
	3	M	10	1	3	LEV, OXC
	4	F	30	6	1–2	LEV
	5	M	15	2	12–24	LEV, VPA
	6	F	7	4	Total 1	LEV
	7	M	22	1	4–6	OXC
	8	F	26	3	Total 2	LEV
	9	M	12	3	2	LEV
	10	M	39	15	3	VPA
FCD	11	M	41	28	Total 3	LEV, CBZ
	12	F	31	20	60	OXC, LEV, TPM
	13	M	30	4	0–1	LEV, OXC
	14	M	40	4	4–6	LEV, OXC
	15	F	20	5	12	OXC
	16	F	24	10	4–5	LEV
	17	M	34	28	3–4	OXC
	18	F	31	10	24–36	OXC
	19	F	10	3	36	LEV
	20	F	27	13	120	LEV, OXC
PMG	21	M	31	4	132	VPA
	22	M	18	10	2–3	OXC
	23	F	21	13	12	OXC
	24	M	19	0.5	Total 2	OXC
	25	F	12	4	2–6	LEV
	26	M	38	17	48	OXC, LEV
	27	F	10	1	10	OXC
	28	M	8	3	52	OXC, LEV
	29	M	15	7	24–36	LEV, OXC

MCDs, malformations of cortical development; GMH, gray matter heterotopia; M, male; LEV, levetiracetam; OXC, oxcarbazepine; VPA, valproate; F, female; FCD, focal cortical dysplasia; CBZ, carbamazepine; TPM, topiramate; PMG, polymicrogyria.

Table 2 The measurements of spectral quality and tissue fractions in measured VOIs in participants with MCDs and HC

Parameters	HC (n=25)	MCDs_NACS (n=29)	MCDs_lesion (n=29)	$P_{HC\ vs.\ MCDs\_NACS}$	$P_{HC\ vs.\ MCDs\_lesion}$	$P_{MCDs\_NACS\ vs.\ MCDs\_lesion}$
FWHM	0.042±0.005	0.045±0.012	0.050±0.014	0.896	0.074	0.038*
SNR	26.20±5.72	27.62±8.70	24.03±8.88	0.477	0.286	0.001*
GMV/total volume	0.40±0.11	0.27±0.15	0.22±0.13	<0.001*	<0.001*	0.050
WMV/total volume	0.51±0.18	0.67±0.17	0.70±0.16	0.002*	<0.001*	0.705
GMV/(GMV + WMV)	0.46±0.16	0.29±0.17	0.24±0.15	<0.001*	<0.001*	0.112
WMV/(GMV + WMV)	0.54±0.16	0.71±0.17	0.76±0.15	<0.001*	<0.001*	0.112

Data are presented as the mean ± standard deviation. *, P<0.05. VOIs, volumes of interest; MCDs, malformations of cortical development; HC, healthy controls; NACS, normal-appearing contralateral side; FWHM, full width at half maximum; SNR, signal-to-noise ratio; GMV, gray matter volume; WMV, white matter volume.

Table 3 Metabolite concentrations (mmol/kg wet weight)

Metabolites	HC (n=25)	MCDs (n=29)		GMH (n=10)		FCD (n=10)		PMG (n=9)	
		NACS	Lesion	NACS	Lesion	NACS	Lesion	NACS	Lesion
Ins	4.82±0.49	4.77±0.85	5.67±1.53*†	4.86±1.05	5.19±1.77	4.91±0.95	6.06±1.56*†	4.55±0.39	5.77±1.22†
NAA	7.47±0.50	7.40±1.05	6.79±1.00*†	7.09±1.12	6.38±1.14*‡	7.65±0.83	6.81±0.91*†	7.51±1.17	7.22±0.83
Cho	1.38±0.10	1.52±0.29*	1.63±0.39*	1.48±0.27	1.52±0.32	1.61±0.29	1.89±0.50†	1.45±0.23	1.51±0.19
Cr	5.57±0.46	5.81±0.87	6.11±0.94*	5.75±1.22	5.57±0.91	5.92±0.72	6.25±0.86†	5.80±0.53	6.56±0.86*†
Glx	10.15±1.19	10.20±2.59	10.36±1.67	10.93±3.35	10.22±1.48	9.86±2.54	9.96±1.85	9.79±1.52	10.95±1.70†

Data are expressed as the group mean ± standard deviation. *, P<0.05 in comparison with the HC; †, P<0.05 in pairwise comparison with the corresponding NACS; ‡, P<0.05 in comparison between GMH_lesion and PMG_lesion. HC, healthy controls; MCDs, malformations of cortical development; NACS, normal-appearing contralateral side; GMH, gray matter heterotopia; FCD, focal cortical dysplasia; PMG, polymicrogyria; Ins, myoinositol; NAA, N-acetyl aspartate; Cho, choline; Cr, creatine; Glx, glutamate + glutamine.

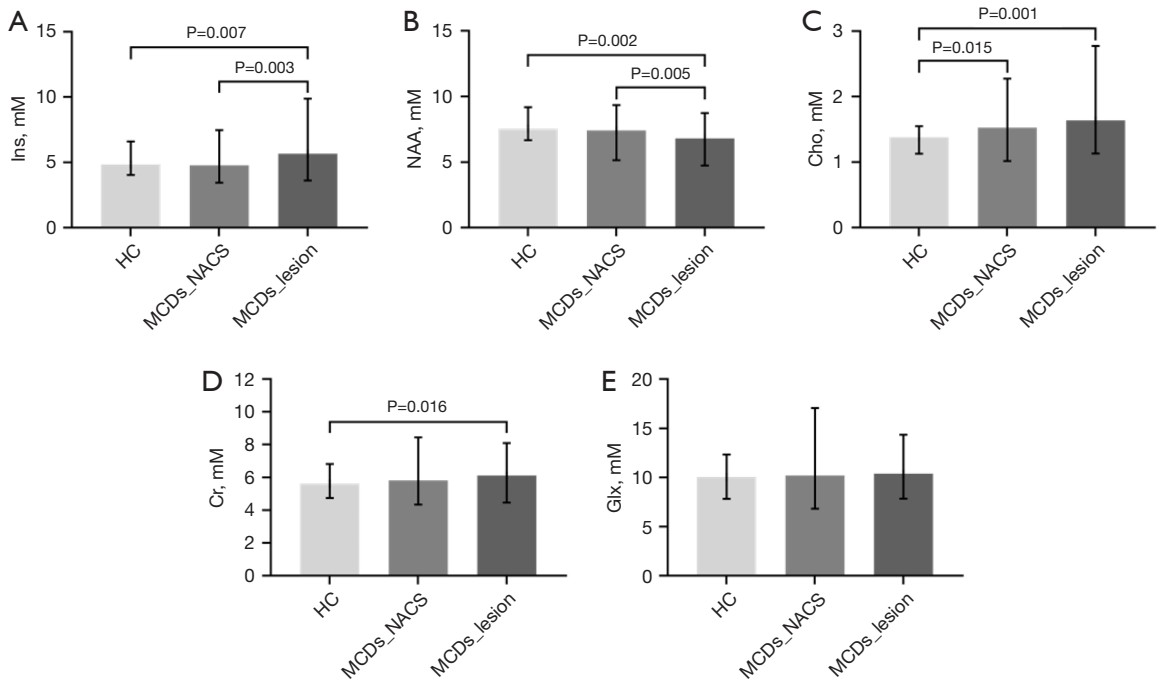

Figure 3 Comparison of metabolic concentrations between the patients with MCDs and the HC. Metabolites include Ins (A), NAA (B), Cho (C), Cr (D), and Glx (E). The upper edge and whisker of the rectangle represent the mean and range, respectively. HC, healthy controls; MCDs, malformations of cortical development; NACS, normal-appearing contralateral side; Ins, myoinositol; NAA, N-acetyl aspartate; Cho, choline; Cr, creatine; Glx, glutamate + glutamine.

the NACS and lesion (all P values >0.05). In the patients with FCD, the NAA concentration was decreased (lesion *vs.* NACS: 6.81±0.91 *vs.* 7.65±0.83, P=0.042), while Cho (lesion *vs.* NACS: 1.89±0.50 *vs.* 1.61±0.29, P=0.041), Cr (lesion *vs.* NACS: 6.25±0.86 *vs.* 5.92±0.72, P=0.046), and Ins (lesion *vs.* NACS: 6.06±1.56 *vs.* 4.91±0.95, P=0.012) concentrations were higher in the lesion than in the NACS. In the patients with PMG, Ins (lesion *vs.* NACS: 5.77±1.22 *vs.* 4.55±0.39, P=0.021), Cr (lesion *vs.* NACS: 6.56±0.86 *vs.* 5.80±0.53, P=0.017), and Glx (lesion *vs.* NACS: 10.95±1.70 *vs.* 9.79±1.52, P=0.043) concentrations were significantly higher in the lesion than in the NACS.

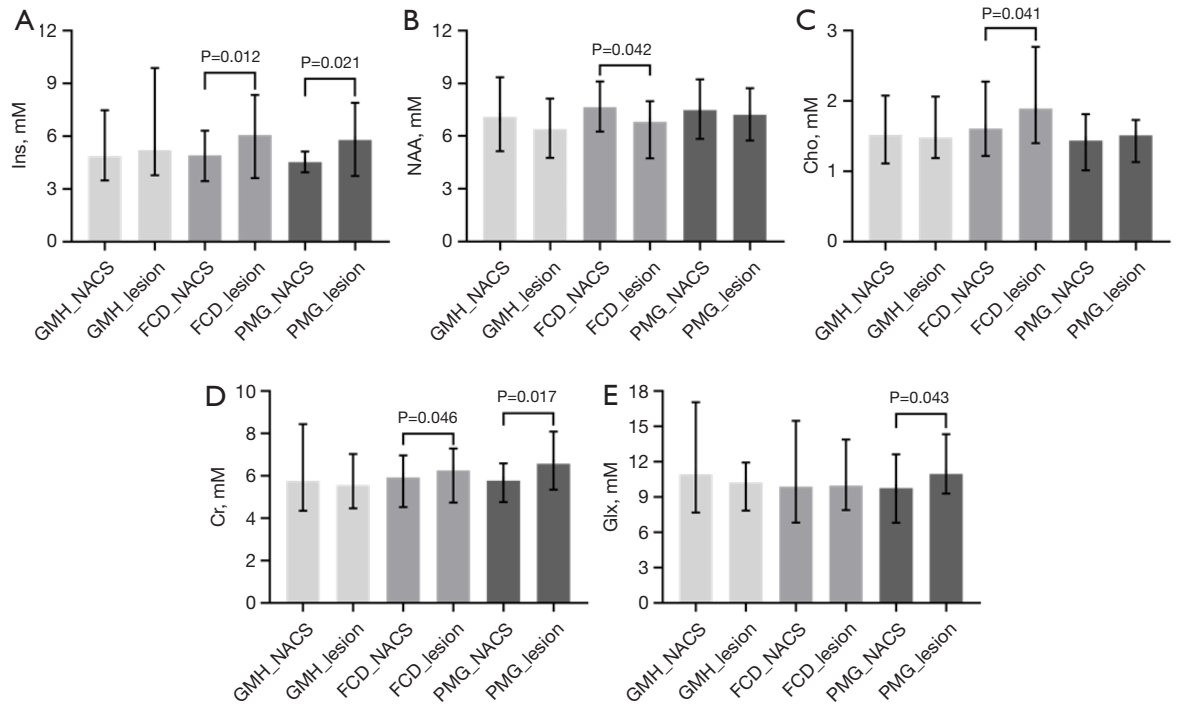

Figure 4 Comparison of metabolic concentrations between the lesion and the corresponding NACS in each MCDs subtype. Metabolites include Ins (A), NAA (B), Cho (C), Cr (D), and Glx (E). The upper edge and whisker of the rectangle represent the mean and range, respectively. GMH, gray matter heterotopia; NACS, normal-appearing contralateral side; FCD, focal cortical dysplasia; PMG, polymicrogyria; Ins, myoinositol; NAA, N-acetyl aspartate; Cho, choline; Cr, creatine; Glx, glutamate + glutamine; MCDs, malformations of cortical development.

Metabolic differences among the three MCDs subgroups and the HC group

The multiple comparison results are shown in *Figure 5*. In the comparison between the HC group and the NACS of MCDs subgroups (HC *vs.* GMH_NACS *vs.* FCD_NACS *vs.* PMG_NACS), there was no significant difference in metabolite concentrations (all P values >0.05).

For the comparison among the HC group and the lesion of MCDs subgroups (HC *vs.* GMH_lesion *vs.* FCD_lesion *vs.* PMG_lesion), in the GMH subgroup, only the NAA of lesion was lower than that of the HC group (GMH_lesion *vs.* HC: 6.38±1.14 *vs.* 7.47±0.50, P=0.001). In the FCD subgroup, the NAA concentration was lower (FCD_lesion *vs.* HC: 6.81±0.91 *vs.* 7.47±0.50, P=0.030), while the Ins concentration was higher in lesion than in the HC group (FCD_lesion *vs.* HC: 6.06±1.56 *vs.* 4.82±0.49, P=0.019). Although Cho and Cr concentrations were increased in lesion when compared to HC, the differences were not significant after correction for multiple comparisons (P=0.010 and P=0.007 before correction, and P=0.058 and P=0.810 after correction, respectively). In the PMG subgroup, the Cr concentration of the lesion was higher than that of the HC (PMG_lesion *vs.* HC: 6.56±0.86 *vs.* 5.57±0.46, P=0.021). Ins and Cho concentrations were higher in lesion than in HC, but there was no statistically significant difference after correction for multiple comparisons (P=0.048 and P=0.012 before correction, and P=0.052 and P=0.362 after correction, respectively). Furthermore, the NAA concentration of the GMH lesion was significantly lower than that of the PMG lesion (GMH_lesion *vs.* PMG_lesion: 6.38±1.14 *vs.* 7.22±0.83, P=0.024).

Correlations between metabolite concentrations and seizure frequency or duration

Among all metabolites, only the Cr concentration in the MCDs lesions was positively correlated with the seizure frequency [r=0.411; 95% confidence interval (CI): 0.0411–0.682; P=0.027; *Figure 6*). However, as shown in *Figure 6*,

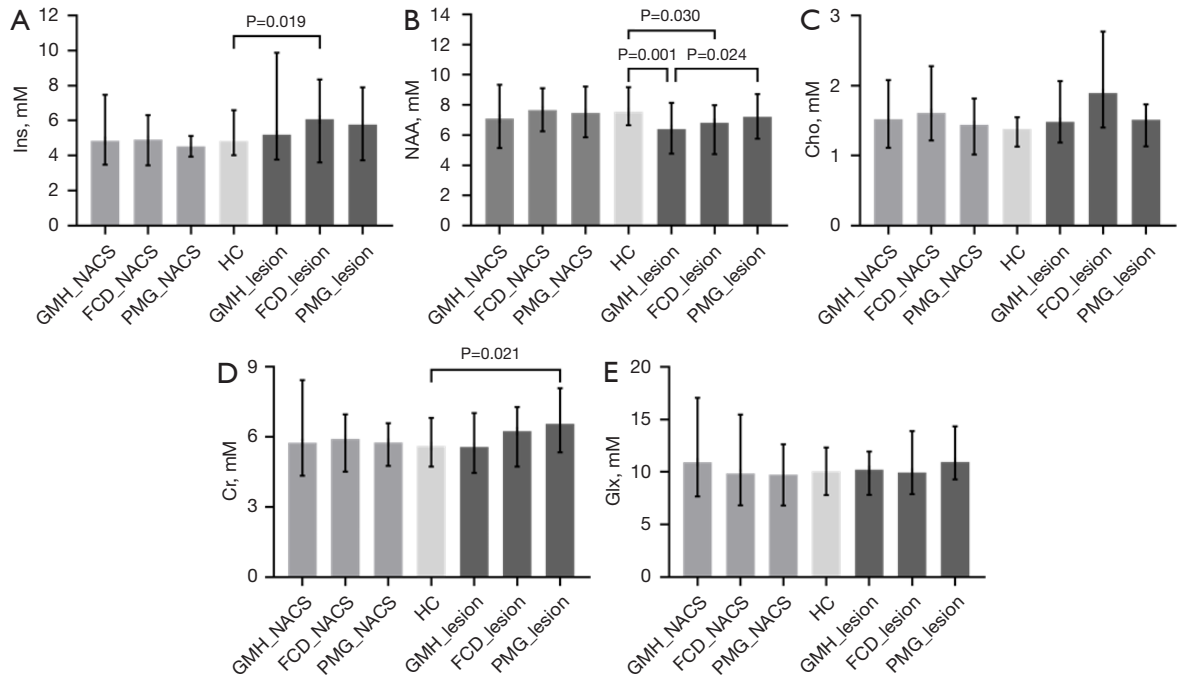

Figure 5 Comparison of metabolic concentrations among the HC and the three subgroups of MCDs. Metabolites include Ins (A), NAA (B), Cho (C), Cr (D), and Glx (E). The upper edge and whisker of the rectangle represent the mean and range, respectively. GMH, gray matter heterotopia; NACS, normal-appearing contralateral side; FCD, focal cortical dysplasia; PMG, polymicrogyria; Ins, myoinositol; NAA, N-acetyl aspartate; Cho, choline; Cr, creatine; Glx, glutamate + glutamine; HC, healthy controls; MCDs, malformations of cortical development.

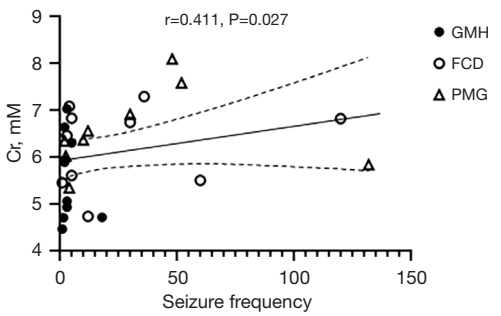

Figure 6 The Cr concentration of the MCDs lesions is positively correlated with the seizure frequency. The solid line represents the linear regression line, and the dotted line represents the 95% CI of the linear fit. GMH, gray matter heterotopia; FCD, focal cortical dysplasia; PMG, polymicrogyria; Cr, creatine; MCDs, malformations of cortical development; CI, confidence interval.

we found that most of scatter points were outside the 95% CI of the linear fit, and the scatter points distributed on both sides of the linear regression line were mainly from FCD and PMG lesions. There were no significant correlations between the metabolite concentrations in MCDs lesions and seizure duration or between the metabolite concentrations of lesions and seizure frequency or duration in any MCDs subtype (all P values >0.05).

Discussion

The primary findings of this study are as follows: (I) there were lower NAA and higher Ins concentrations in MCDs lesions than in the NACS of MCDs and HC, higher Cho and Cr concentrations in MCDs lesions than in HC, and higher Cho concentration in the NACS of MCDs than in HC. (II) Each MCDs subtype exhibited characteristic metabolic alterations. GMH had no metabolic abnormalities except for decreased NAA. FCD showed more abnormal metabolite concentrations, particularly decreased NAA and increased Ins in the lesion compared to HC and NACS. Unlike other subtypes, PMG showed no remarkable alteration in NAA concentration but did have increased Glx concentration. (III) Correlation analysis revealed that the Cr concentration of MCDs lesions was positively correlated

with seizure frequency.

In patients with MCDs, NAA reduction and Ins increase were noticed in MCDs lesions when compared to HC and NACS. In previous studies, the decreases of NAA concentration (9-13,25) and NAA/Cr ratio (6,8,14,15) were the major abnormalities identified in MCDs lesions, which is in agreement with our results. NAA is mainly synthesized in neuronal mitochondria, and NAA changes have been linked to the function, viability, and quantity of the bodies, axons, dendrites, and synapses of neurons (26). Decreased NAA concentration is generally indicative of neuronal dysfunction or loss of neurons. However, the histopathologic findings of patients with MCDs showed an increased or normal neuronal density in lesions (27,28). In an immunocytochemical study of rats with neocortical malformations and epilepsy, there was a delay in the developmental switch from α1 to α2 subunits in γ-aminobutyric acid A ($GABA_A$) receptors of neocortical pyramidal cells in the lesioned cortex and a delay in the expression of the N-methyl-D-aspartate receptor subunit 2A (NR2A), suggesting functional immaturity of the neurons (29). Additionally, NAA has been proven to be related to adenosine triphosphate (ATP) metabolism via participating in a mechanism that enhances mitochondrial energy production from glutamate (Glu) (26). Thus, NAA reduction might represent the abnormalities in neuronal maturation, dysfunction of neurons, or impairment in neuronal energy metabolism associated with MCDs lesions and epileptic activity. Ins is an organic osmolyte, largely originates from glial cells, and is commonly identified as a glia-specific marker (30). Therefore, an increase in Ins concentration might reflect glial proliferation.

Our study also found that the metabolic differences between MCDs lesions and HC were greater than those between MCDs lesions and NACS of MCDs, with higher Cho and Cr concentrations in MCDs lesions than in HC. In the comparison of NACS of MCDs and HC, NACS had a higher Cho concentration than HC. These findings indicate that NACS may also be affected by lesions. Cho is an important constituent of the phospholipid metabolism of cell membranes, and Cho concentration primarily provides information regarding membrane integrity and turnover (30), cell density (31), and the degree of myelination (32). An elevated Cho concentration might suggest increased membrane turnover and immature neuronal tissue. In the patients with MCDs, epileptogenic activity could be explained by abnormalities in tissue architecture and function, with consequent abnormal synaptic activity and circuitry, as well as unstable membrane excitability (33). Previous MRS studies have demonstrated that the metabolic conditions in the structurally normal-appearing regions surrounding MCDs lesions (9,14) or in the opposite hemisphere (8,9,15) were disrupted, indicating widespread impairment of cerebral function. However, these studies reported decreased NAA concentration or NAA/Cr ratio (9,15) and decreased Cho/Cr ratio (8) in the NACS spectra of patients with MCDs as compared with the controls. This discrepancy may be attributed to different MRS postprocessing and analysis technologies or the heterogeneity of the patient population. From previous studies (8,14), it could be speculated that NAA abnormality was most evident in the center of MCDs lesion and gradually decreased with the distance from the lesion. Whereas, in the MCDs subgroups of our study, there were no metabolic differences between the NACS and HC. We consider that this may be due to the small sample size of each subgroup. Functional MRI research has revealed brain topological network disruptions and local or large-scale functional connectivity anomalies in patients with MCDs (34). Other neuroimaging modalities, including single-photon emission computed tomography (SPECT) (35), positron emission tomography (PET) (36), and DTI (16), have provided indirect or direct evidence to support the hypothesis that the abnormalities of neuronal function or micro-dysgenesis were beyond the limits of the visualized MCDs lesions. These findings may help to explain why it is more difficult for patients with apparently focal MCDs to become seizure-free after surgical removal of the visible lesion than patients with other pathologies (18). The newly proposed surgical management of MCDs with pharmaco-resistant epilepsy, stereotactic surgery, targets the crucial nodes of the epileptogenic network and will become an important development direction (37). Moreover, in the VOIs, gray matter and white matter may contain different concentrations of metabolites. In our study, the differences in the tissue fractions and spectral quality in measured VOIs between the MCDs lesions and the HC or NACS may be attributable to variations in the GMV/WMV ratio in the lesion areas, the variability and complexity of the lesions, and the different locations of the VOIs.

GMH is a collection of neurons and glia in abnormal locations and is secondary to the arrest of the migration of neurons. In the comparison among HC, and the lesion and NACS of GMH, the only metabolic difference was a significantly lower NAA concentration in GMH lesions than in HC. In the past MRS studies of GMH, the NAA

signal (13,25) or NAA/Cr ratio (6-8,14) ranged from normal to below normal, suggesting that the functional maturity of neurons varies from case to case. Histological findings of some studies indicated that heterotopic lesions contain immature neurons and incomplete differentiation related to abnormal patterns of synaptic connections (38,39). Therefore, less NAA may point to the majority of heterotopic neurons being at an immature stage and dysfunctional despite the presence of a large quantity of neurons in the GMH areas. The subsequently improper cerebral connectivity resulting from heterotopic neurons may help to trigger epilepsy (14). Moreover, our study, in line with other studies (6,7,25), didn't find obvious abnormality in the concentrations of Ins, Cho, or Cr in GMH. However, in the research of Munakata *et al.* (6) on band heterotopia (also referred to as double cortex), the Cho/Cr ratio was significantly increased while NAA/Cr ratio was not changed in laminar heterotopias. Histologically, the heterotopic band consists of randomly arranged but relatively well-differentiated pyramidal cells (6). Considering the subcategories of the GMH, primarily subependymal, subcortical, and band heterotopias (1), we speculate that the maturity of neuronal function may also differ among the three GMH subtypes, which may be further investigated via MRS or histopathological study.

FCD is a later cortical developmental disorder secondary to abnormal postmigrational development and may be accompanied by the presence or absence of abnormal cell types (19). In the present study, compared to the NACS, FCD lesions showed reduced NAA and elevated Ins, Cho, and Cr. Compared to HC, FCD lesions had decreased NAA and increased Ins. Although the Cho and Cr concentrations of FCD lesions were significantly higher than those of HC, neither of them passed correction for multiple comparisons. Our results are in accordance with previous reports on small groups of patients with FCD, which reported a reduction in NAA (10,12,25) or NAA/Cr ratio (10,40) within FCD lesions. In a previous study by Tan *et al.* (13), significantly increased Ins and Cr concentrations were observed in the DOPM subgroup (including FCD and PMG), but not in the DOM subgroup (including GMH) when compared to HC or NACS. According to the clinicopathologic spectrum of FCD, the ILAE proposed a three-tiered classification system (types I–III) to distinguish isolated FCDs (19), with FCD type II (characterized by varying degrees of cortical dyslamination and dysmorphic neurons without or with balloon cells) being the most common type (19). In our study, three patients with FCD confirmed by postoperative pathology were FCD type II. The metabolic disturbances in FCD type II could mainly be explained by disorganization of tissue architecture with dysplastic neurons, incomplete differentiated cells, and gliosis, which is an additional feature of FCD lesions (41).

In the clinical performance, we found that patients with FCD had a longer epilepsy duration than patients with GMH, and the metabolite abnormalities in Ins, Cho, and Cr of FCD lesions were more obvious than those of GMH lesions. In addition to considering the pathophysiological differences between the two subtypes, whether chronic epilepsy caused by longer seizure duration affects metabolite concentrations requires to be considered. However, no correlation was found between seizure duration and metabolite concentrations in this study.

PMG is characterized by overfolding of the cerebral cortex and abnormal cortical layering (2). In our cohorts, the PMG lesions presented higher Ins, Cr, and Glx concentrations than the NACS of PMG, and a higher Cr concentration than the HC; specifically, the NAA was not significantly changed in PMG lesions. In the studies of Widjaja *et al.* (7) and Li *et al.* (14) of 21 and three patients with PMG, respectively, the NAA/Cr ratio in PMG was also not significantly reduced when compared with HC. The timing of the insult in PMG is the final stages of neuronal migration and the early phases of cortical organization, and the neurons are deemed to be mature, with normal cellular structure and the presence of synaptic integrity (7,14). This may account for our findings in which the NAA concentration in GMH lesions was also lower than that in PMG lesions. Cr is thought to be mainly found in glial cells (42). The PMG is usually related to diffuse or patchy astrogliosis or dysmyelination in the white matter (3), which explains the increased Cr found in the PMG lesions. A notable finding in our study was that Glx concentration of PMG lesions was higher than that of the NACS. On conventional or edited MRS, Glu and glutamine (Gln) have overlapping peaks that are difficult to distinguish and are therefore generally reported as a combined signal of Glx (43). Glu is a primary excitatory neurotransmitter in the brain and plays a major role in the initiation and spread of seizure activity (44). The Glu-Gln cycle between neurons and glia is a key mechanism for the control of glutamatergic neurotransmission (45). The average seizure frequency of patients with PMG was also higher than that of patients with FCD or GMH, with the difference for the latter being significant. Hence, an elevated Glx concentration may be a result of recurrent seizures and energy depletion leading to

partial failure of neurotransmitter cycling and subsequent neurotransmitter accumulation in the surrounding astrocytes (as Gln) or within the neuronal cytoplasm (as Glu).

In the correlation analysis, there was a positive correlation between Cr concentration and seizure frequency in patients with MCDs (r=0.411; P=0.027). This is consistent with the findings of Tan *et al.* (13) on MCDs and Tschampa *et al.* (12) on FCD, who reported a weak to moderate positive correlation between Cr concentration of the lesions and seizure frequency. The Cr peak in MRS is a composite of Cr and phosphocreatine that interconvert to regenerate ATP, thus acting as a short-term energy "buffer" for the cell (46). It was reported that elevation in Cr concentration may reflect disrupted energy metabolism (hypermetabolism in lesions) because a more metabolically active cell reasonably requires a greater capacity to regenerate ATP (46). While Cr is found in both neurons and glial cells, its concentration is highest in astrocytes (42). An increase of Cr concentration in patients with MCDs lesions and intrinsic epileptogenicity could indicate hypermetabolism and astrogliosis (12). Nevertheless, the correlation between Cr concentration of MCDs lesions and seizure frequency in this study was weak, and most of the scatter points were outside the 95% CI of the linear fit (*Figure 6*), which may be attributed to the small sample size. This finding needs to be verified in future studies with larger-scale cohorts or results from multiple centers. The epilepsy duration did not correlate with metabolic concentrations in MCDs or three subtypes, which is in accordance with the literatures (8,12). However, other researchers also did not find any of the aforementioned clinical correlations of metabolites in patients with MCDs (8,11). These discrepancies may be due to heterogeneity of the MCDs population or the presence of various MCDs subtypes. As in the results of correlation analysis, the points scattered on both sides of the fitted line were mainly from FCD and PMG lesions.

There are some limitations to this study which should be mentioned. First, our study was inevitably affected by the small sample population of patients with MCDs and each subtype. Second, although the differences in age were nonsignificant among the adult HC group and three subtypes, 10 patients were younger than 18 years of age (age range, 7–15 years). To counteract this, we compared the lesion to the NACS in the same patient. Third, we could not identify the relative contributions of antiepileptic medications. Valproate treatment has been reported to be associated with increased Glx and reduced Ins concentrations (47). In our cohort, however, the number of patients treated with valproate was relatively small, and the Ins concentration in the lesions had a tendency to increase instead of decrease. Fourth, some prefrontal metabolite levels, especially the Cr, have been reported to be affected by the phases of the menstrual cycle (48). Control for the phases of the menstrual cycle should be implemented in future studies of brain metabolite dysregulation in patients with MCDs.

Conclusions

Our study demonstrated neurometabolic heterogeneity among different MCDs subtypes. Compared with HC and/or NACS, GMH was characterized only by decreased NAA concentration, FCD by decreased NAA concentration and increased Ins concentration, and PMG by elevated Glx concentration and normal NAA concentration. Therefore, we speculate that when MCDs are analyzed as a whole, the heterogeneity of various subtypes might be indiscernible. One possible recommendation is that each MCDs subtype is studied separately to elucidate its specific neurobiochemical mechanisms.

Acknowledgments

Funding: This work was supported by the National Natural Science Foundation of China (Nos. 82271961, 82302160, 81820108018, and 82027808) and the Sichuan Provincial Foundation of Science and Technology (No. 2022YFS0073).

Footnote

Reporting Checklist: The authors have completed the STROBE reporting checklist. Available at https://qims.amegroups.com/article/view/10.21037/qims-23-552/rc

Conflicts of Interest: All authors have completed the ICMJE uniform disclosure form (available at https://qims.amegroups.com/article/view/10.21037/qims-23-552/coif). The authors have no conflicts of interest to declare.

Ethical Statement: The authors are accountable for all aspects of the work in ensuring that questions related to the accuracy or integrity of any part of the work are appropriately investigated and resolved. The study was approved by the local ethical committee of the West China Hospital of Sichuan University. All participants or the legal

guardians of younger patients provided written informed consent for enrollment in this study. The study was conducted in accordance with the Declaration of Helsinki (as revised in 2013).

References

1. Battal B, Ince S, Akgun V, Kocaoglu M, Ozcan E, Tasar M. Malformations of cortical development: 3T magnetic resonance imaging features. World J Radiol 2015;7:329-35.
2. Guerrini R, Dobyns WB. Malformations of cortical development: clinical features and genetic causes. Lancet Neurol 2014;13:710-26.
3. Leventer RJ, Guerrini R, Dobyns WB. Malformations of cortical development and epilepsy. Dialogues Clin Neurosci 2008;10:47-62.
4. Barkovich AJ, Guerrini R, Kuzniecky RI, Jackson GD, Dobyns WB. A developmental and genetic classification for malformations of cortical development: update 2012. Brain 2012;135:1348-69.
5. Castillo M, Kwock L, Mukherji SK. Clinical applications of proton MR spectroscopy. AJNR Am J Neuroradiol 1996;17:1-15.
6. Munakata M, Haginoya K, Soga T, Yokoyama H, Noguchi R, Nagasaka T, Murata T, Higano S, Takahashi S, Iinuma K. Metabolic properties of band heterotopia differ from those of other cortical dysplasias: a proton magnetic resonance spectroscopy study. Epilepsia 2003;44:366-71.
7. Widjaja E, Griffiths PD, Wilkinson ID. Proton MR spectroscopy of polymicrogyria and heterotopia. AJNR Am J Neuroradiol 2003;24:2077-81.
8. Simone IL, Federico F, Tortorella C, De Blasi R, Bellomo R, Lucivero V, Carrara D, Bellacosa A, Livrea P, Carella A. Metabolic changes in neuronal migration disorders: evaluation by combined MRI and proton MR spectroscopy. Epilepsia 1999;40:872-9.
9. Woermann FG, McLean MA, Bartlett PA, Barker GJ, Duncan JS. Quantitative short echo time proton magnetic resonance spectroscopic imaging study of malformations of cortical development causing epilepsy. Brain 2001;124:427-36.
10. Mueller SG, Laxer KD, Barakos JA, Cashdollar N, Flenniken DL, Vermathen P, Matson GB, Weiner MW. Metabolic characteristics of cortical malformations causing epilepsy. J Neurol 2005;252:1082-92.
11. Simister RJ, McLean MA, Barker GJ, Duncan JS. Proton magnetic resonance spectroscopy of malformations of cortical development causing epilepsy. Epilepsy Res 2007;74:107-15.
12. Tschampa HJ, Urbach H, Träber F, Sprinkart AM, Greschus S, Malter MP, Surges R, Gieseke J, Block W. Proton magnetic resonance spectroscopy in focal cortical dysplasia at 3T. Seizure 2015;32:23-9.
13. Tan Q, Liu W, Wan X, Wang W, Su X, Sun H, Zhang S, Yue Q. Quantitative 1H-MRS reveals metabolic difference between subcategories of malformations of cortical development. Neuroradiology 2021;63:1539-48.
14. Li LM, Cendes F, Bastos AC, Andermann F, Dubeau F, Arnold DL. Neuronal metabolic dysfunction in patients with cortical developmental malformations: a proton magnetic resonance spectroscopic imaging study. Neurology 1998;50:755-9.
15. Leite CC, Lucato LT, Sato JR, Valente KD, Otaduy MC. Multivoxel proton MR spectroscopy in malformations of cortical development. AJNR Am J Neuroradiol 2007;28:1071-5; discussion 1076-7.
16. Eriksson SH, Rugg-Gunn FJ, Symms MR, Barker GJ, Duncan JS. Diffusion tensor imaging in patients with epilepsy and malformations of cortical development. Brain 2001;124:617-26.
17. Vitali P, Minati L, D'Incerti L, Maccagnano E, Mavilio N, Capello D, Dylgjeri S, Rodriguez G, Franceschetti S, Spreafico R, Villani F. Functional MRI in malformations of cortical development: activation of dysplastic tissue and functional reorganization. J Neuroimaging 2008;18:296-305.
18. Raymond AA, Fish DR, Sisodiya SM, Alsanjari N, Stevens JM, Shorvon SD. Abnormalities of gyration, heterotopias, tuberous sclerosis, focal cortical dysplasia, microdysgenesis, dysembryoplastic neuroepithelial tumour and dysgenesis of the archicortex in epilepsy. Clinical, EEG and neuroimaging features in 100 adult patients. Brain 1995;118:629-60.
19. Blümcke I, Thom M, Aronica E, Armstrong DD, Vinters HV, Palmini A, et al. The clinicopathologic spectrum of focal cortical dysplasias: a consensus classification proposed

by an ad hoc Task Force of the ILAE Diagnostic Methods Commission. Epilepsia 2011;52:158-74.
20. Baker EH, Basso G, Barker PB, Smith MA, Bonekamp D, Horská A. Regional apparent metabolite concentrations in young adult brain measured by (1)H MR spectroscopy at 3 Tesla. J Magn Reson Imaging 2008;27:489-99.
21. Haga KK, Khor YP, Farrall A, Wardlaw JM. A systematic review of brain metabolite changes, measured with 1H magnetic resonance spectroscopy, in healthy aging. Neurobiol Aging 2009;30:353-63.
22. Nagae-Poetscher LM, Bonekamp D, Barker PB, Brant LJ, Kaufmann WE, Horská A. Asymmetry and gender effect in functionally lateralized cortical regions: a proton MRS imaging study. J Magn Reson Imaging 2004;19:27-33.
23. Provencher SW. Estimation of metabolite concentrations from localized in vivo proton NMR spectra. Magn Reson Med 1993;30:672-9.
24. Hammen T, Hildebrandt M, Stadlbauer A, Doelken M, Engelhorn T, Kerling F, Kasper B, Romstoeck J, Ganslandt O, Nimsky C, Blumcke I, Doerfler A, Stefan H. Non-invasive detection of hippocampal sclerosis: correlation between metabolite alterations detected by (1)H-MRS and neuropathology. NMR Biomed 2008;21:545-52.
25. Kaminaga T, Kobayashi M, Abe T. Proton magnetic resonance spectroscopy in disturbances of cortical development. Neuroradiology 2001;43:575-80.
26. Moffett JR, Ross B, Arun P, Madhavarao CN, Namboodiri AM. N-Acetylaspartate in the CNS: from neurodiagnostics to neurobiology. Prog Neurobiol 2007;81:89-131.
27. Battaglia G, Arcelli P, Granata T, Selvaggio M, Andermann F, Dubeau F, Olivier A, Tampieri D, Villemure JG, Avoli M, Avanzini G, Spreafico R. Neuronal migration disorders and epilepsy: a morphological analysis of three surgically treated patients. Epilepsy Res 1996;26:49-58.
28. Kuzniecky R, Hetherington H, Pan J, Hugg J, Palmer C, Gilliam F, Faught E, Morawetz R. Proton spectroscopic imaging at 4.1 tesla in patients with malformations of cortical development and epilepsy. Neurology 1997;48:1018-24.
29. Hablitz JJ, DeFazio RA. Altered receptor subunit expression in rat neocortical malformations. Epilepsia 2000;41 Suppl 6:S82-5.
30. Ranjeva JP, Confort-Gouny S, Le Fur Y, Cozzone PJ. Magnetic resonance spectroscopy of brain in epilepsy. Childs Nerv Syst 2000;16:235-41.
31. Miller BL, Chang L, Booth R, Ernst T, Cornford M, Nikas D, McBride D, Jenden DJ. In vivo 1H MRS choline: correlation with in vitro chemistry/histology. Life Sci 1996;58:1929-35.
32. Hida K, Kwee IL, Nakada T. In vivo 1H and 31P NMR spectroscopy of the developing rat brain. Magn Reson Med 1992;23:31-6.
33. Sarnat HB. Cerebral dysplasias as expressions of altered maturational processes. Can J Neurol Sci 1991;18:196-204.
34. Hong SJ, Bernhardt BC, Gill RS, Bernasconi N, Bernasconi A. The spectrum of structural and functional network alterations in malformations of cortical development. Brain 2017;140:2133-43.
35. Iannetti P, Spalice A, Atzei G, Boemi S, Trasimeni G. Neuronal migrational disorders in children with epilepsy: MRI, interictal SPECT and EEG comparisons. Brain Dev 1996;18:269-79.
36. Richardson MP, Koepp MJ, Brooks DJ, Fish DR, Duncan JS. Benzodiazepine receptors in focal epilepsy with cortical dysgenesis: an 11C-flumazenil PET study. Ann Neurol 1996;40:188-98.
37. Bourdillon P, Rheims S, Catenoix H, Montavont A, Ostrowsky-Coste K, Isnard J, Guénot M. Malformations of cortical development: New surgical advances. Rev Neurol (Paris) 2019;175:183-8.
38. Hannan AJ, Servotte S, Katsnelson A, Sisodiya S, Blakemore C, Squier M, Molnár Z. Characterization of nodular neuronal heterotopia in children. Brain 1999;122:219-38.
39. Chevassus-au-Louis N, Represa A. The right neuron at the wrong place: biology of heterotopic neurons in cortical neuronal migration disorders, with special reference to associated pathologies. Cell Mol Life Sci 1999;55:1206-15.
40. Colon AJ, Hofman P, Ossenblok PP, Jansen JF, Ter Beek LC, Berting R, Stam CJ, Boon P. MRS-lateralisation index in patients with epilepsy and focal cortical dysplasia or a MEG-focus using bilateral single voxels. Epilepsy Res 2010;89:148-53.
41. Urbach H, Scheffler B, Heinrichsmeier T, von Oertzen J, Kral T, Wellmer J, Schramm J, Wiestler OD, Blümcke I. Focal cortical dysplasia of Taylor's balloon cell type: a clinicopathological entity with characteristic neuroimaging and histopathological features, and favorable postsurgical outcome. Epilepsia 2002;43:33-40.
42. Pan JW, Kuzniecky RI. Utility of magnetic resonance spectroscopic imaging for human epilepsy. Quant Imaging Med Surg 2015;5:313-22.
43. Novotny EJ Jr, Fulbright RK, Pearl PL, Gibson KM, Rothman DL. Magnetic resonance spectroscopy of neurotransmitters in human brain. Ann Neurol 2003;54 Suppl 6:S25-31.

44. Chapman AG. Glutamate and epilepsy. J Nutr 2000;130:1043S-5S.
45. Shen J, Rothman DL. Magnetic resonance spectroscopic approaches to studying neuronal: glial interactions. Biol Psychiatry 2002;52:694-700.
46. Meyer EJ, Kirov II, Tal A, Davitz MS, Babb JS, Lazar M, Malaspina D, Gonen O. Metabolic Abnormalities in the Hippocampus of Patients with Schizophrenia: A 3D Multivoxel MR Spectroscopic Imaging Study at 3T. AJNR Am J Neuroradiol 2016;37:2273-9.
47. Garcia M, Huppertz HJ, Ziyeh S, Buechert M, Schumacher M, Mader I. Valproate-induced metabolic changes in patients with epilepsy: assessment with H-MRS. Epilepsia 2009;50:486-92.
48. Hjelmervik H, Hausmann M, Craven AR, Hirnstein M, Hugdahl K, Specht K. Sex- and sex hormone-related variations in energy-metabolic frontal brain asymmetries: A magnetic resonance spectroscopy study. Neuroimage 2018;172:817-25.

Cite this article as: Pu H, Wang L, Liu W, Tan Q, Wan X, Wang W, Su X, Sun H, Zhang S, Yue Q, Gong Q. Metabolic heterogeneity in different subtypes of malformations of cortical development causing epilepsy: a proton magnetic resonance spectroscopy study. Quant Imaging Med Surg 2023;13(12):8625-8640. doi: 10.21037/qims-23-552

